Journal of Computer-Aided Molecular Design, 5 (1991) 213–234
ESCOM

J-CAMD 108

A molecular model for the active site of *S*-adenosyl-L-homocysteine hydrolase

Jerry C. Yeh[a], Ronald T. Borchardt[a,*] and Angelo Vedani[b]

[a]*Department of Pharmaceutical Chemistry and* [b]*Department of Chemistry, The University of Kansas, Lawrence, KS 66045, U.S.A.*

Received 23 January 1990
Accepted 16 July 1990

Key words: Molecular modeling; Molecular mechanics; Energy minimization; Protein–ligand binding

SUMMARY

S-adenosyl-L-homocysteine hydrolase (AdoHcy hydrolase, EC 3.3.1.1), a specific target for antiviral drug design, catalyzes the hydrolysis of AdoHcy to adenosine (Ado) and homocysteine (Hcy) as well as the synthesis of AdoHcy from Ado and Hcy. The enzyme isolated from different sources has been shown to contain tightly bound NAD^+.

Based on the 2.0 Å-resolution X-ray crystal structure of dogfish lactate dehydrogenase (LDH), which is functionally homologous to AdoHcy hydrolase, and the primary sequence of rat liver AdoHcy hydrolase, we have derived a molecular model of an extended active site for AdoHcy hydrolase. The computational mutation was performed using the software MUTAR (Yeh et al., University of Kansas, Lawrence), followed by molecular mechanics optimizations using the programs AMBER (Singh et al., University of California, San Francisco) and YETI (Vedani, University of Kansas). Solvation of the model structure was achieved by use of the program SOLVGEN (Jacober, University of Kansas); 56 water molecules were explicitly included in all refinements. Some of these may be involved in the catalytic reaction.

We also studied a model of the complex of AdoHcy hydrolase with NAD^+, as well as the ternary complexes of the enzyme, NAD^+, and substrate or inhibitor molecules. Our refined model is capable of explaining part of the redox reaction catalyzed by AdoHcy hydrolase and has been used to differentiate the relative binding strength of inhibitors.

INTRODUCTION

The enzyme *S*-adenosyl-L-homocysteine hydrolase (AdoHcy hydrolase, EC 3.3.1.1) catalyzes both the hydrolysis of AdoHcy to adenosine (Ado) and homocysteine (Hcy) and the synthesis of AdoHcy from Ado and Hcy (Scheme 1). AdoHcy hydrolase isolated from different sources has been shown to contain tightly bound NAD^+[1]. Inhibitors of AdoHcy hydrolase appear to produce different effects on NAD^+ in the inhibitory reactions, either by release of the cofactor or by

*To whom correspondence should be addressed.

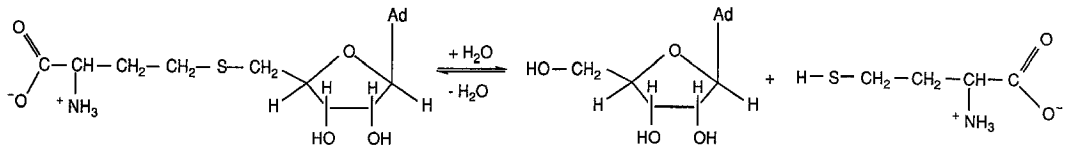

Scheme 1. Reaction catalyzed by AdoHcy hydrolase.

its reduction to NADH [2,3]. Because of its ability to regulate biological transmethylation reactions, which are essential in the maturation of certain eukaryotic and viral messenger RNA molecules, AdoHcy hydrolase has become a specific target for antiviral drug design [4]. Neplanocin A (NpcA), which is one of the most potent inhibitors of AdoHcy hydrolase [5], has two pronounced biological effects: antiviral activity and cytotoxicity [6]. In addition to its inhibitory effects against AdoHcy hydrolase, NpcA is also a substrate for adenosine kinase and adenosine deaminase. Our laboratory has hypothesized that the antiviral effects of NpcA are mediated by the inhibitory effects of the drug on cellular AdoHcy hydrolase, and that its cytotoxic effects are due to its metabolism by adenosine kinase to NpcA triphosphate with subsequent metabolism to *S*-neplanocyl-L-methionine by methionine adenosyltransferase [4,7]. Aristeromycin (AristM) is another potent inhibitor of AdoHcy hydrolase [8]. Like NpcA, AristM has also been reported to be a substrate of adenosine deaminase and adenosine kinase [9]. A series of NpcA and AristM analogs [10–12 and Wolfe et al., J. Med. Chem., submitted] have been synthesized in this laboratory in an attempt to obtain monofunctional antiviral agents (specific inhibitors of AdoHcy hydrolase) with a minimum of other metabolic effects (i.e., substrate activity with adenosine deaminase and adenosine kinase).

It is well known that lactate dehydrogenase (LDH), malate dehydrogenase, glyceraldehyde-3-phosphate dehydrogenase, and liver alcohol dehydrogenase (LADH) contain a similar 3D structure in their NAD^+ binding domains even though their primary sequences and the locations of these binding domains within the primary sequences are quite different [13,14]. The dehydrogenases catalyze redox reactions that involve the removal of a proton (H^+) from a hydroxyl group and transfer of a hydride ion (H^-) from the carbon atom that bears the hydroxyl group to the C4 atom in the nicotinamide (Nic) portion of NAD^+ [14]. Thus, structural and electronic factors must govern the recognition and binding of NAD^+ in such a manner that the Nic moiety is oriented properly with respect to the substrate in the active site [14]. It has also been observed that AdoHcy hydrolase catalyzed a similar redox reaction utilizing the interconversion of NAD^+ and NADH (Scheme 2) [15]. A model of the enzyme at the molecular level would be of great value in elucidating the role of NAD^+ in the catalytic cycle and its role in the mechanism of enzyme inactivation by inhibitors.

Since the tertiary structure of AdoHcy hydrolase is presently unknown, the immediate goal of this study was to generate a model of the 3D structure of AdoHcy hydrolase by computational modification of a known functionally homologous protein structure, namely LDH. Subsequently, molecular modeling techniques [16–18] were used to examine the binding of small molecules (both substrates and inhibitors) and to gain a better understanding of structural requirements for substrate and inhibitor binding and the catalytic mechanism of AdoHcy hydrolase. Finally, infor-

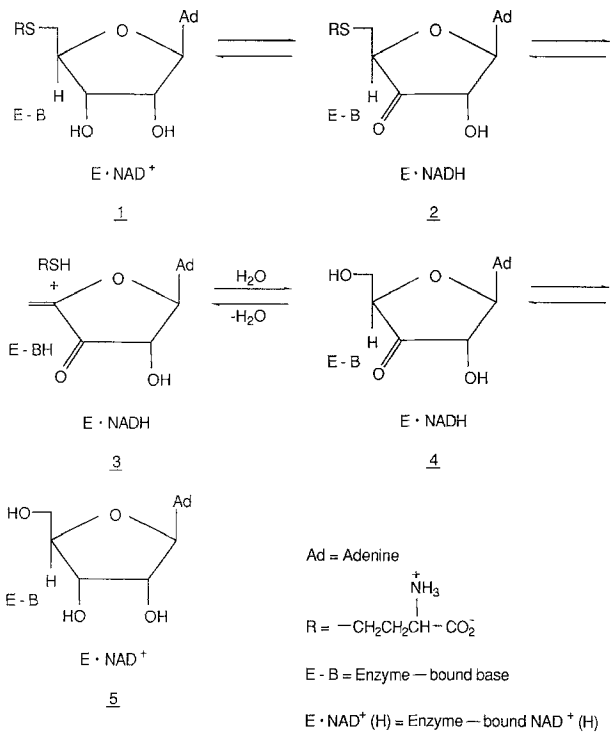

Scheme 2. Mechanism of action of AdoHcy hydrolase.

mation obtained from the model will be used to design more potent inhibitors for further antiviral study, and the experimental data will be used to modify the initial model.

METHODS

Our strategy in deriving a 3D model for the enzyme AdoHcy hydrolase included the following steps: (1) generation of a model for the 3D structure of the NAD^+ binding domain of AdoHcy hydrolase based on the X-ray crystal structure of LDH using the program MUTAR (Scheme 3); (2) docking of NAD^+ into its binding domain using interactive computer-graphics techniques; (3) extending the mutation beyond the NAD^+ binding domain to generate a potential active site; and (4) docking substrates and inhibitors into the active site. All structures used in the modeling were subjected to energy minimization.

The known 3D structure of a protein can be more readily used to derive a model for another protein if the target protein (of which only the primary sequence is known) shows a high sequential homology. Starting from a well-refined structure of the reference protein, the nonidentical sequences are altered by means of molecular modeling to obtain a crude starting model of the target protein. The mutated structure is subsequently relaxed by energy minimization techniques [19] to ensure a structurally and energetically realistic model.

The putative NAD^+ binding region of AdoHcy hydrolase (residues 213–244) from rat liver has 48% homology to the NAD^+ binding region of LDH (residues 22–51) (Table 1) [20]; a somewhat

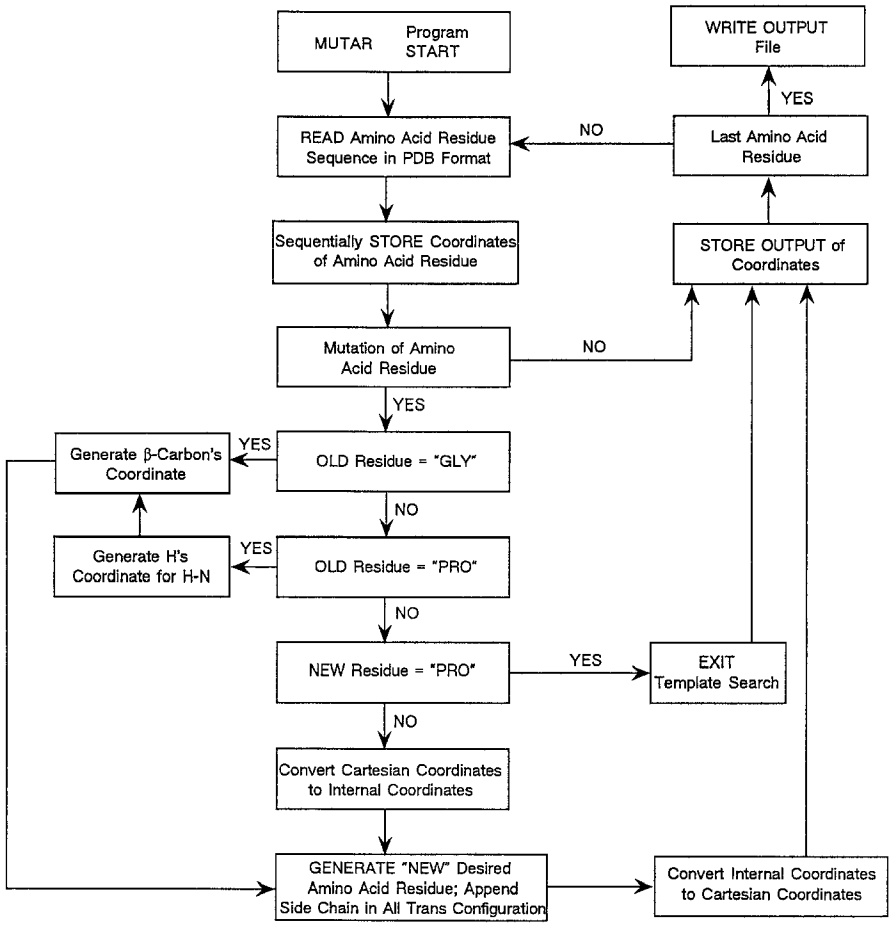

Scheme 3. Flow chart of MUTAR.

lower homology is found for other dehydrogenases [21]. Recently, it has been postulated that residues 213–244 might bind the adenosine diphosphate portion of NAD^+ in AdoHcy hydrolase [22].

(1) Refinement of the LDH structure

To achieve the overall goal stated above, we began to construct the NAD^+ binding domain of AdoHcy hydrolase using its primary sequence and the tertiary structure of LDH [23]. The starting coordinates of the dogfish LDH apoenzyme [24] were retrieved from the Brookhaven Protein Data Bank (BPDB) [25]. The 2.0-Å X-ray crystal structure of LDH has an R factor of 43%; therefore, we preferred to optimize the LDH structure by means of molecular mechanics techniques. These energy calculations were performed with version 3.0 of the program AMBER [26] and with version 4.3 of the program YETI [27] on a μ-VAX II computer at the Biographics Laboratory and a VAX 8650 computer at the Academic Computing Services of the University of Kansas.

The refinements of the LDH structure included 2553 heavy atoms (C, N, O, S) and 572 polar H atoms attached to O, N, and S atoms of the protein. H atoms attached to C atoms were in-

TABLE 1
THE AMINO ACID SEQUENCE[a] OF A: LDH [20] AND B: AdoHcy HYDROLASE [21]

```
        22                                                  30
A       LYS Ile Thr VAL VAL  -  GLY Cys GLY Ala VAL GLY Met Ala CYS
B       LYS Val Ala VAL VAL Ala GLY Tyr GLY Asp VAL GLY Lys Gly CYS
        213                     220
                          40                                      50
A       ALA Ile Ser Ile Leu Met Lys Asp Leu Ala Asp Glu Val Ala Leu
B       ALA Gln Ala Leu Arg Gly Phe Gly Ala Arg Val Ile Ile Thr Glu
                230                                 240
                                                    60
A       Val ASP Val Met Glu Asp Lys Leu Lys Gly  -  GLU Met Met Asp
B       Ile ASP Pro Ile Asn Ala Leu Gln Ala Ala Met GLU Gly Tyr Glu
                                    250
                               70
A       Leu Gln His Gly Ser Leu Phe Leu His Thr Ala Lys ILE Val Ser
B       Val Thr Thr Met Asp Glu Ala Cys Lys Glu Gly Asn ILE Phe Val
                260                                 270
         80                                                 90
A       Gly Lys Asp Tyr Ser VAL Ser Ala Gly Ser Lys Leu Val Val Ile
B       Thr Thr Thr Gly Cys VAL Asp Ile Ile Leu Gly Arg His Phe Glu
                                    280
                          100
A       Thr Ala Gly Ala Arg Gln Gln Glu Gly Glu Ser Arg Leu Asn Leu
B       Gln Met Lys Asp Asp Ala Ile Val Cys Asn Ile Gly His Phe Asp
                290                                 300
        110                                                120
A       VAL Gln Arg Asn VAL Asn Ile Phe Lys Phe Ile Ile Pro Asn Ile
B       VAL Glu Ile Asp VAL Lys Trp Leu Asn Glu Asn Ala Val Glu Lys
                                    310
                          130
A       VAL Lys His Ser PRO Asp Cys Ile Ile Leu Val Val Ser ASN Pro
B       VAL Asn Ile Lys PRO Gln Val Asp Arg Tyr Leu Leu Lys ASN Gly
                320                                 330
        140                                                150
A       Val Asp Val Leu Thr Tyr Val Ala Trp Lys LEU Ser Gly LEU Pro
B       His Arg Ile Ile Leu Leu Ala Glu Gly Arg LEU Val Asn LEU Gly
                                    340
                          160                       165
A       Met His Arg Ile Ile Gly SER Gly Cys Asn Leu Asp SER Ala Arg
B       Cys Ala Met Gly His Pro SER Phe Val Met Ser Asn SER Phe Thr
                350                                 358
        170
A       Phe Arg Tyr Leu Met Gly Glu Arg LEU Gly Val HIS Ser Cys Ser
B       Asn Gln Val Met Ala Gln Ile Glu LEU Trp Thr HIS Pro Asp Lys
                                    370
                          190
A       Gly Val Gly Trp VAL Ile Gly Gln His Gly Asp Ser Val Pro Ser
B       Tyr Pro Val Gly VAL His Phe Leu Pro Lys Lys Leu Asp Glu Ala
                380                                 390
        200                                                210
A       VAL Trp Ser Gly Met Trp Asn Ala LEU Lys Glu Leu His Pro Glu
B       VAL Ala Glu Ala His Leu Gly Lys LEU Asn Val Lys Leu Thr Lys
                                    400
                          220
A       LEU Gly THR Asn LYS Asp Lys GLN Asp Trp Lys Lys Leu His Lys
B       LEU  -  THR Glu LYS Gln Ala GLN Tyr Leu Gly Met Pro Ile Asn
                    410                                     420
        230                                            239
A       Asp Val Val Asp Ser Ala Tyr Glu Val Ile
B       Gly Pro Phe Lys Pro Asp His Tyr Arg Tyr
                                        430
```

[a]Identical residues are capitalized.

cluded within united atoms. All 42 experimentally determined water molecules were also included in the energy minimization. A full relaxation of the protein and solvent was performed by AMBER, which uses a combined steepest-descent (50 steps)/conjugate-gradient (450 steps) minimizer in Cartesian coordinate space. Convergence criteria for all AMBER refinements were set at 0.09 kcal/(mol·Å) for first derivative RMS values; the cut-off distance for non-bonded interactions was set at 10.0 Å. The program YETI also uses a steepest-descent (5–20 steps)/conjugate-gradient (50–200 steps) minimizer, but performs the optimizations in a mixed internal/Cartesian coordinate space. In contrast to AMBER, YETI does not alter the backbone conformation. Also, bond lengths and bond angles are not varied during the refinements. The main advantage of YETI is that its force-field energy expression includes directional terms for hydrogen-bond and salt linkages (Eqs. 1 and 2). The distance-dependent dielectric model was used in AMBER and YETI refinements and the dielectric parameter was set equal to 2.0. In YETI, the degrees of freedom include all protein side-chain torsions, torsions, rotations, and translations of the coenzyme, substrates and inhibitors as well as translations and rotations of all water molecules. Using smooth cut-off criteria [28] of 9.5/10.0 Å (switch-on, switch-off) for electrostatic interactions, 6.5/7.0 Å for van der Waals interactions, and 5.5/6.0 Å for hydrogen bonds, the initial list of non-bonded interactions numbered about 240 000. Convergence criteria for the energy refinements were set at 0.025 kcal/(mol·deg) for torsional, 0.050 kcal/(mol·deg) for rotational, and 0.750 kcal/mol·Å) for translational RMS first derivatives, respectively. Apart from the treatment of hydrogen bonds and metal–ligand interactions, the YETI force field for non-bonded interactions is identical to the AMBER force field.

$$E_{total} = \sum_{bonds} K_r(r - r_{eq})^2 + \sum_{angles} K_\theta - \theta_{eq})^2 + \sum_{dihedrals} \frac{V_n}{2}\{1 + \cos(n\,\phi - \gamma)\}$$

$$+ \sum_{i<j}\left(\frac{A_{ij}}{R_{ij}^{12}} - \frac{B_{ij}}{R_{ij}^{6}} + \frac{q_i q_j}{\varepsilon R_{ij}}\right) + \sum_{H\text{-}bonds}\left(\frac{C_{ij}}{R_{ij}^{12}} - \frac{D_{ij}}{R_{ij}^{10}}\right) \tag{1}$$

Eq. 1. AMBER force field equation [cf. Ref. 26].

$$E_{total} = \sum_{dihedrals} \frac{V_n}{2}\{1 + \cos(n\phi - \gamma)\} + \sum_{i<j} \frac{1}{4\pi\varepsilon_o} \cdot \frac{q_i q_j}{D(r) r_{ij}} + \sum_{i<j} \frac{A_{ij}}{r_{ij}^{12}} - \frac{C_{ij}}{r_{ij}^{6}}$$

$$+ \sum_{H\text{-}bonds}\left(\frac{A'}{r_{H\text{-}Acc}^{12}} - \frac{C'}{r_{H\text{-}Acc}^{10}}\right) \cdot \cos^2(\theta_{Don\text{-}D\text{-}Acc}) \cdot \cos^4(\omega_{H\text{-}Acc\text{-}LP})$$

$$+ \sum_{ML\ bonds}\left(\frac{A''}{r_{M\cdot\cdot L}^{12}} - \frac{C''}{r_{M\cdot\cdot L}^{10}}\right) \cdot \prod_{indep.\ angles} \cos^2(\psi_{L\text{-}M\text{-}L} - \psi_o) \tag{2}$$

Eq. 2. YETI force field equation [cf. Ref. 27].

(2) Mutation of protein structure

To test the robustness of our approach, we used the β–α–β fold of the NAD^+ binding domain in the enzymes LDH [24] and LADH [29] as an example for computational mutation since the X-ray crystal structures of both enzymes are available. The amino acid sequence of the β–α–β fold (Table 2) in LDH and LADH has a 42% homology. The goal of this mutation was to obtain a model of β–α–β fold for LADH from LDH using MUTAR, and then to compare this model structure with the β–α–β fold of the X-ray crystal structure of LADH as deposited in BPDP. During the computational mutation from LDH to LADH, it was necessary to delete residue Leu^{44} from LDH. After the mutation, deletion, and molecular mechanics refinements using the programs YETI and AMBER, the model of β–α–β fold for LADH was compared with the β–α–β fold in the 2.9 Å-resolution X-ray crystal structure of the complex of holo-LADH, NAD^+ and DMSO, Brookhaven entry 6ADH. The model structure showed an RMS shift of 1.03 Å for all α-carbon positions (Fig. 1), ranging from 0.09 Å to 2.47 Å. The uncertainty in atomic positions (σ) of the LADH X-ray crystal structure, derived from the isotropic temperature factor, is about 0.5 Å. Thus, the RMS shift reported here falls in the range of 2σ. This is in agreement with the maximum shift of 1 Å–1.5 Å suggested by Stewart et al. [19] as a criterion for testing the accuracy of a modeling approach in predicting the structure of a protein using a related structure. Finally, the difference in force-field energy of the refined model and X-ray structures is about 5 kcal/mol, which is probably not significant. Therefore, we feel that our approach can provide a certain level of confidence in predicting the structure of the NAD^+ binding domain in AdoHcy hydrolase.

To derive a first model of the 3D structure of AdoHcy hydrolase, all amino acid residues in LDH different from the corresponding ones in AdoHcy hydrolase were replaced using MUTAR. This program generates an extended (all *trans*) side-chain conformation based on the actual main-chain conformation and the position of the β-carbon atom of the residue to be mutated. This procedure cannot be directly applied to modify proline residues. Here, we searched protein structures from the BPDB for matching tri-, tetra-, and pentapeptidic fragments (e.g., Ile-Asp-Pro-Leu) containing proline as the middle residue and the adjacent residues as found in the primary sequence (e.g., Leu-Asp-Pro-Leu) of AdoHcy hydrolase. The coordinates of these fragments were

TABLE 2

THE AMINO ACID SEQUENCE[a] OF THE β–α–β FOLD IN THE NAD^+ BINDING DOMAIN OF A: LDH [20] AND B: LADH [29]

	22								30		
A	Lys	Ile	Thr	VAL	Val	GLY	Cys	Asp	Ala	VAL	GLY
B	Thr	Cys	Ala	VAL	Phe	GLY	Leu	Gly	Gly	VAL	GLY
	194						200				
								40			
A	Met	Ala	Asp	Ala	Ile	Ser	Val	Leu	Met	Lys	Asp
B	Leu	Ser	Val	Ile	Met	Gly	Cys	Lys	Ala	Ala	Gly
						210					
	44						50			53	
A	Leu	ALA	Asp	Glu	Val	Ala	Leu	VAL	ASP	Val	
B	—	ALA	Ala	Arg	Ile	Ile	Gly	VAL	ASP	Ile	
						220				224	

[a]Identical residues are capitalized.

then used as templates for the mutated sequences and inserted using interactive computer graphics techniques (FRODO [30] version 6.6 running on an Evans & Sutherland PS390 graphics display).

To obtain a potential active site (including the NAD^+ binding domain) of AdoHcy hydrolase, the mutation process was divided into two steps: in the first step the mutation included residues 22–164 in LDH; and in the second step the mutation was extended to include residues 165–239. After all mutations were performed, an initial model for the active site of AdoHcy hydrolase including residues 213–431 (corresponding to residues 22–239 in LDH) was obtained. This model was subsequently checked for unfavorable contacts based on interaction energies; these contacts were then relaxed as much as possible by modifying the conformations of the side chains involved. Finally, the structure was refined intermittently by YETI and AMBER.

(3) Docking of coenzyme, substrates, and inhibitors

We used an approach similar to that of Gund and Gund [17] to generate the molecular structures of small molecules which were then docked into the enzyme by means of computer graphics. The position and orientation of the small molecules were chosen to minimize all energetically unfavorable interactions between the small molecules and the enzyme. The coordinates of the small molecules in this particular conformation were then used to calculate the atomic partial charges by use of the semi-empirical molecular orbital calculation program MNDO (as implemented in the program AMPAC [31]). The strategy of our molecular mechanics refinement included: (1) relaxation of the immediate environment of the small molecule (5 Å-zone); and (2) full relaxation of the small molecule–enzyme complex. Details of the docking of individual molecules are described as follows:

(a) Coenzyme. The starting coordinates of the NAD^+ molecule were retrieved from the 2.7 Å-resolution X-ray structure of (*S*)-lac-NAD^+–LDH (pig heart) complex [32]. Since no hydrogen coordinates were reported, their positions were generated based on idealized geometries using the module HYDPOS in YETI. Subsequently, NAD^+ was docked into its binding domain of AdoHcy hydrolase using Asp^{244}, Asn^{331}, and His^{428} as anchor points (Fig. 2). Atomic partial charges of NAD^+ were calculated by AMPAC. Finally, the AdoHcy hydrolase–NAD^+ complex was relaxed by YETI and AMBER using the optimization criteria mentioned above.

(b) Substrates and inhibitors. Using the molecular graphics program package MacroModel [33] (version 2.0), the structures of the substrate AdoHcy [34] and the potent inhibitors NpcA [35] and AristM [36] were retrieved from the Cambridge Structural Database (CSD) [37]. If necessary, unreported H-atom positions were generated. The structures of Ado and Hcy were derived from AdoHcy and the structures of compounds 1 and 2 (Fig. 3) were derived from NpcA. Structures of compounds 3–6 and 8 (Fig. 3) were reformed based on the structure of AristM. All small molecule structures were prerefined by MacroModel using the AMBER force field. In general, a structure with the most reasonable conformation was selected before the docking. Subsequently, substrates and inhibitors were individually docked into the refined active-site model (containing NAD^+) using Asp^{427} as the main anchor point (Fig. 4). Atomic partial charges of substrates and inhibitors were again calculated using AMPAC. Using the same procedure, 3′-ketoNpcA (compound 7a) and 3′-enolNpcA (compound 7b) were derived from NpcA (Fig. 3) and were docked into two separately refined models containing NAD^+ and NADH. In the latter case, Asp^{427} was altered to Ash^{427} (protonated aspartic acid) and was used to anchor both compounds 7a and 7b.

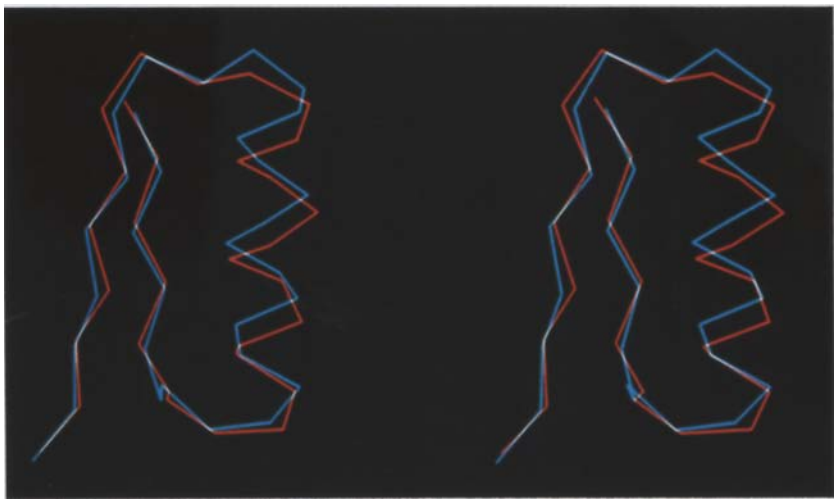

Fig. 1. The α-carbon structure of the β–a–β fold in the NAD^+ binding domain of the LADH model (red) and X-ray crystal structure (blue).

(c) Solvent (H_2O). Internal and some surface waters of AdoHcy hydrolase complexes were generated using the program SOLVGEN [38, 39]. Its algorithm is based on the distance, linearity and lone-pair directionality of hydrogen bonds. SOLVGEN searches the protein for unsaturated hydrogen-bond donors and acceptors, and is capable of generating both internal and surface water molecules. For our model, we were mostly interested in solvent molecules bound within the active site cleft. SOLVGEN identified 56 (in some cases 57) water molecules; 12 of these were bound within the active site (Fig. 5), which was arbitrarily defined as a zone within 8.0 Å of any atom of NpcA.

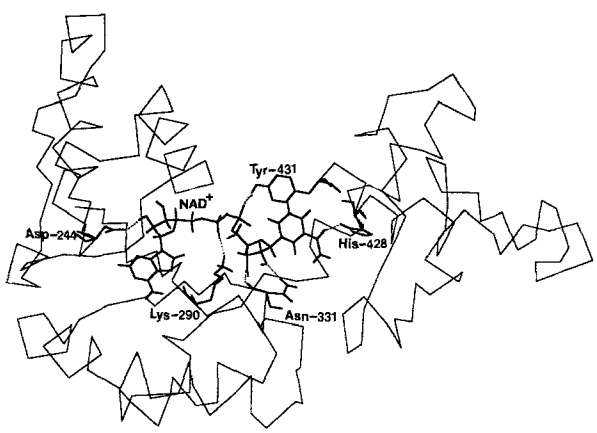

Fig. 2. The α-carbon structure of the NAD^+ binding domain and the active site of the AdoHcy hydrolase model. Dashed lines represent hydrogen bonds between NAD^+ and AdoHcy hydrolase.

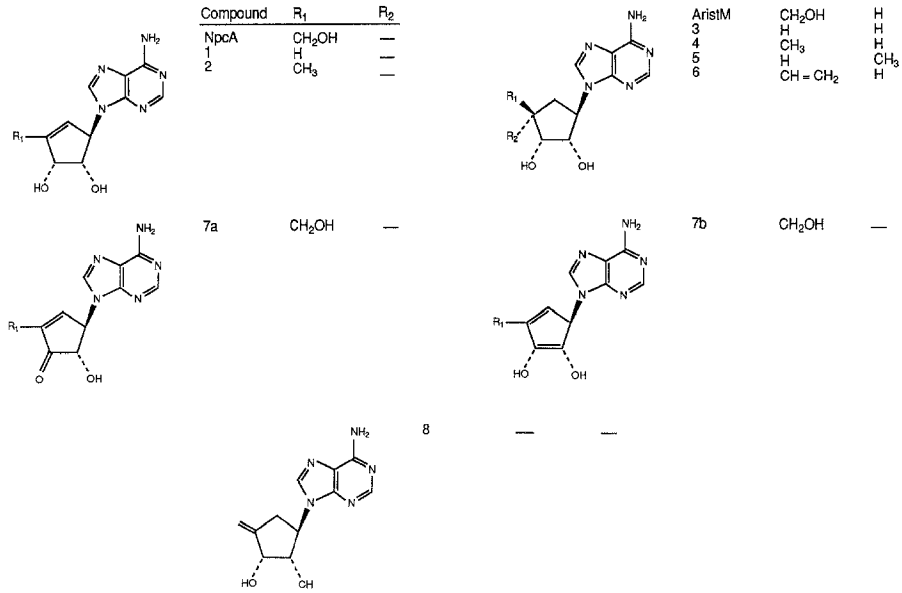

Fig. 3. Structures of potential AdoHcy hydrolase inhibitors.

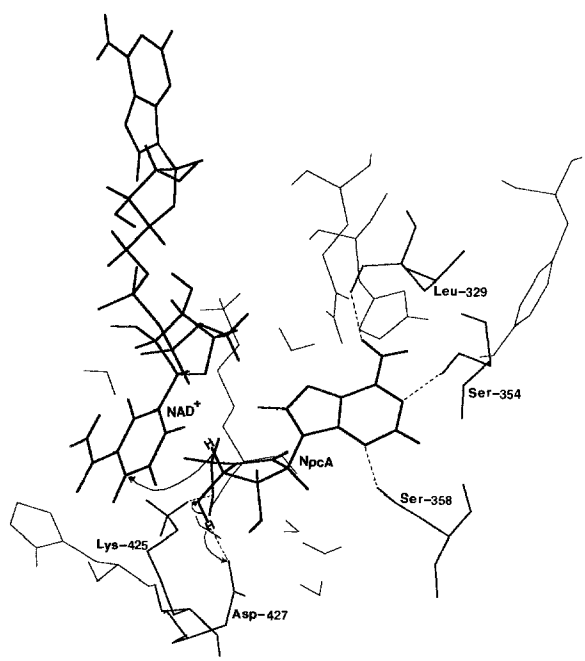

Fig. 4. The potential binding site for NpcA in AdoHcy hydrolase. Dashed lines represent hydrogen bonds between NpcA and amino acid residues in the active site of AdoHcy hydrolase; arrows represent the transfer of H^+ and H^-.

TABLE 3
COMPARISON OF α-CARBON POSITIONS BETWEEN MOLECULAR MECHANICS-REFINED LDH AND MODEL COMPLEXES OF AdoHcy HYDROLASE

	A	B	C	D	E	F
RMS shift (Å)	0.37	0.37	0.63	0.51	0.64	0.63
Max. shift (Å)	1.06	1.06	1.61	1.33	1.63	1.61

A: Model structure of AdoHcy hydrolase; B: Model containing NAD^+; C: Model containing NAD^+ and AdoHcy; D: Model containing NAD^+ and Ado; E: Model containing NAD^+ and Ado and Hcy; F: Model containing NAD^+ and NpcA.

RESULTS

The refined LDH (329 residues) structure displayed an RMS shift of 0.37 Å for all α-carbon atom positions from those of the original X-ray crystal structure of LDH (R factor 0.43). The largest deviation (1.98 Å) occurred at the C-terminal residue Leu^{327}.

It is commonly observed in the homologous modeling of a target protein that insertions and/or deletions of amino acid residues are required. The mutation of LDH to AdoHcy hydrolase required: (1) the insertion of two amino acid residues, Ala^{218} in a loop and Met^{253} in an α-helix; and (2) the deletion of Gly^{216} of LDH in a loop. Without performing the insertions and deletion, the model structure of AdoHcy hydrolase (218 residues) derived from the refined 3D structure of LDH showed an RMS shift of 0.37 Å of all α-carbon atom positions (Table 3). The maximum shift of an α-carbon position, which occurred at Val^{223}, was 1.06 Å. The insertion of Ala^{218}, which

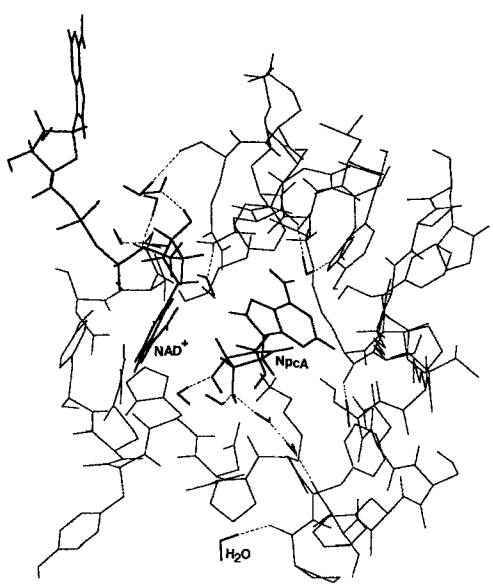

Fig. 5. Twelve water molecules bound in the active site of AdoHcy hydrolase (8.0 Å zone of NpcA). Dashed lines represent hydrogen bonds between H_2O and the active-site model of AdoHcy hydrolase, NpcA and NAD^+; bold lines represent H_2O molecules, NpcA and NAD^+.

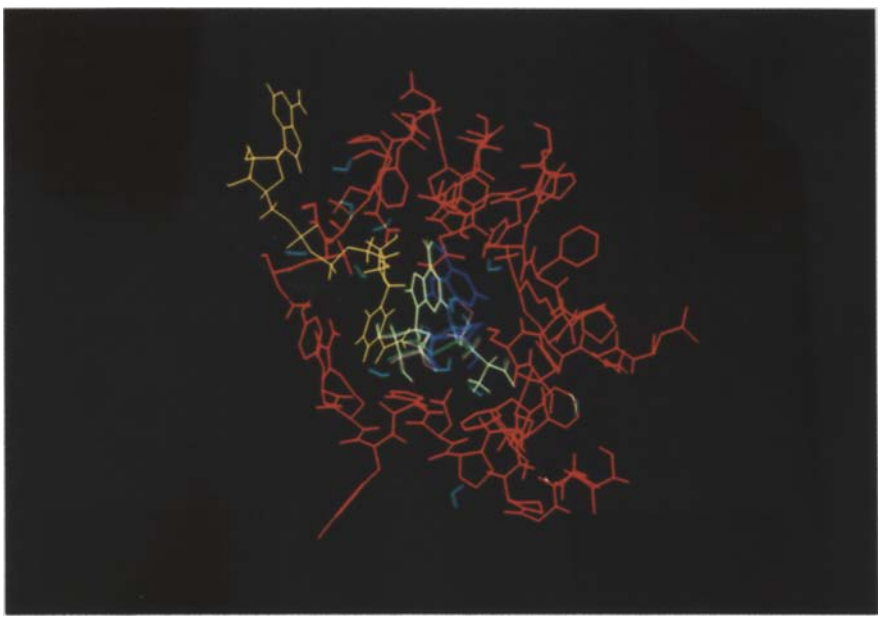

Fig. 6. Binding of AdoHcy (green), Ado (purple), Hcy (purple) and NpcA (deep blue) in the active-site model of the NAD^+ (yellow) form of AdoHcy hydrolase (red) containing some H_2O molecules (light blue).

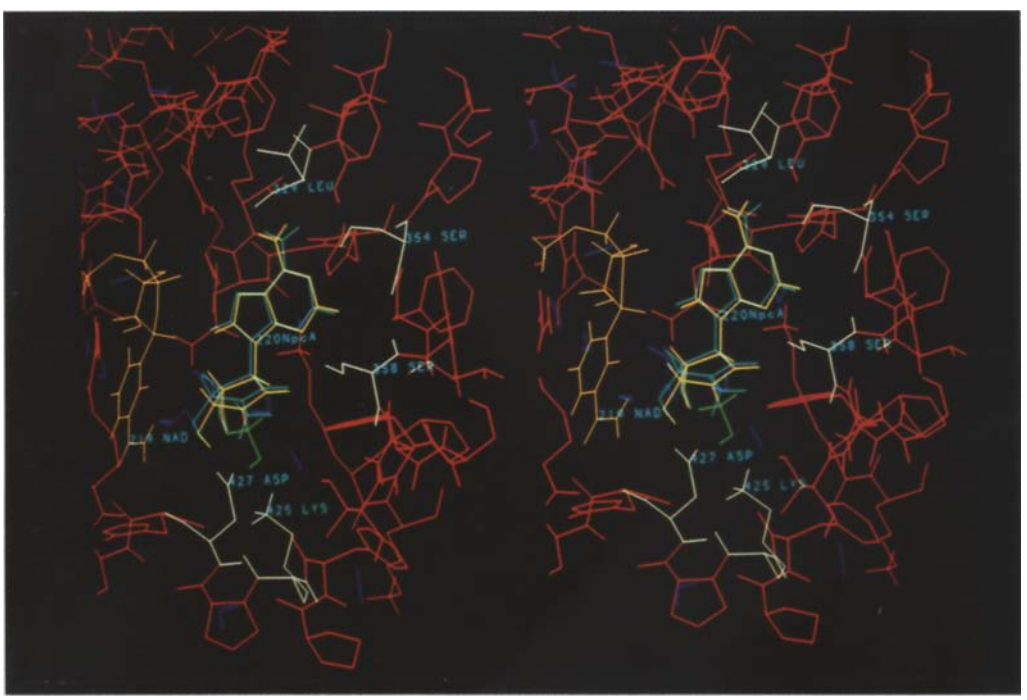

Fig. 7. Binding of NpcA (green), compound 1 (light red), compound 2 (light blue) in the active-site model of AdoHcy hydrolase (red) containing NAD^+ (yellow) and H_2O molecules (blue). Amino acid residues involved in binding of these compounds are white, and light yellow represents the overlap of compound 1 with NpcA.

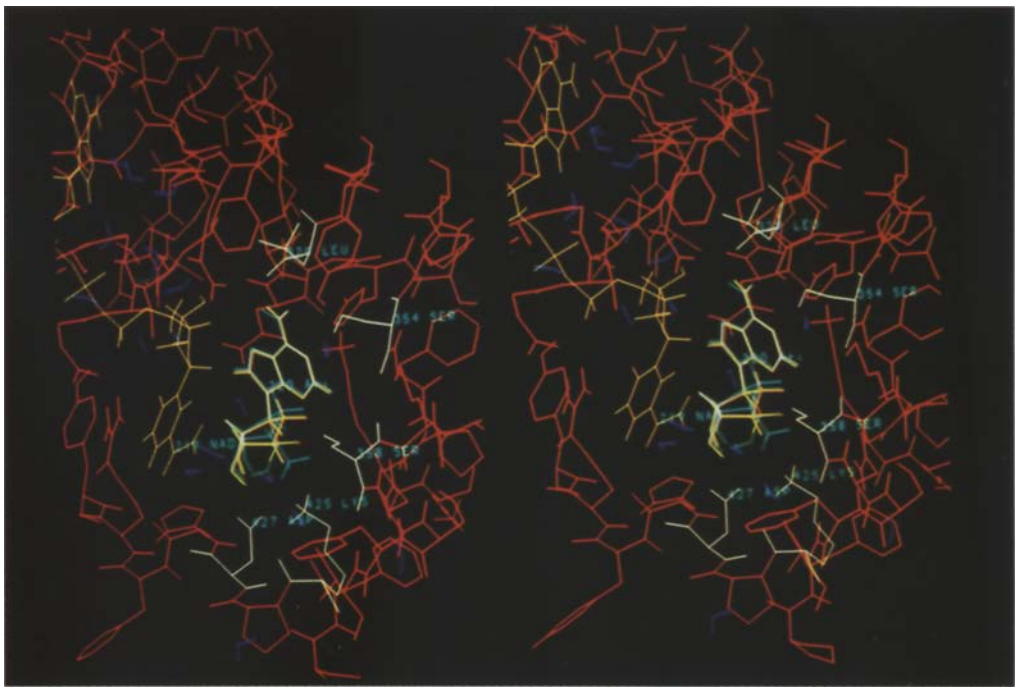

Fig. 8. Binding of AristM (green), compound 3 (light yellow), compound 4 (orange) and compound 5 (light blue) in the active-site model of AdoHcy hydrolase (red) containing NAD^+ (yellow) and H_2O molecules (deep blue). Amino acid residues involved in binding these inhibitors are white.

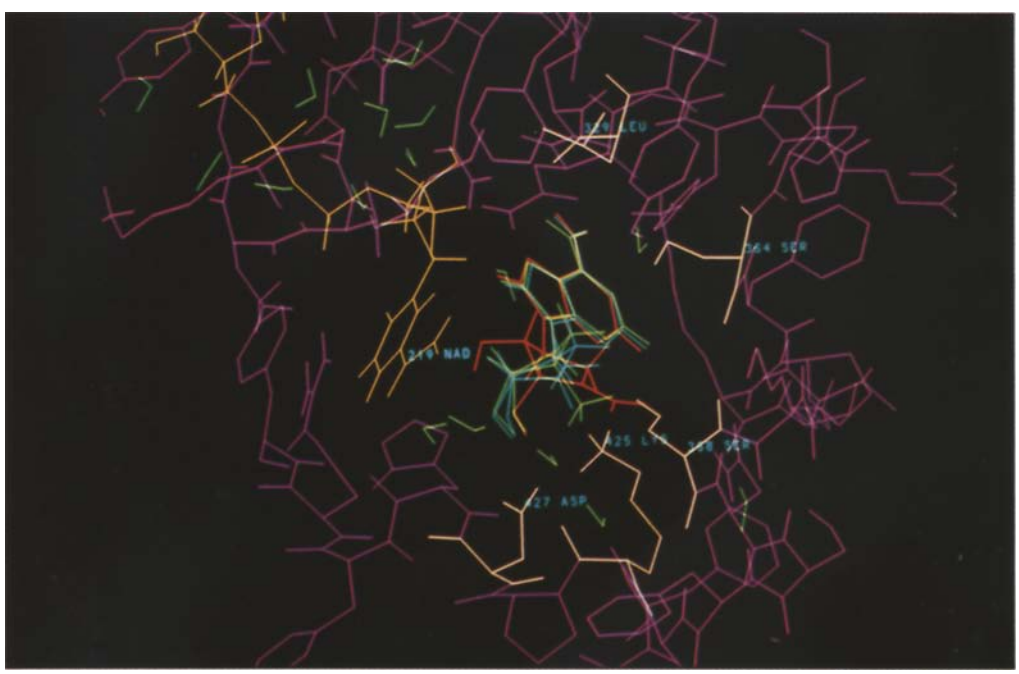

Fig. 9. Binding of compounds 5 (green), 6 (light blue) and 8 (red) in the active-site model of AdoHcy hydrolase (purple) containing NAD^+ (yellow) and H_2O molecules (light green). Amino acid residues involved in binding these inhibitors are pink.

is located in a loop that connects a β-strand and an α-helix in the β–α–β fold, resulted in a large shift (2.87 Å) of the α-carbon atom of Gly^{219}. A major change in the binding of 3′-OH of ribose in the Ado portion of NAD^+ was observed when Ala^{218} was inserted. This caused some uncertainty about the conformation of Ala^{218}, which will require further study. Our model structure did not include the insertion of Met^{253} since it failed to retain the conformation of the helix. A deletion of Gly^{216} in LDH did not cause any significant change in protein backbone conformation.

(1) Binding of coenzyme

Our model structures suggest that NAD^+ binds to its binding domain via hydrogen-bond interactions as well as salt bridges and van der Waals interactions. The binding of the adenine portion is in a nonspecific manner, as observed in other dehydrogenases [13, 14]. In our model, the following hydrogen-bond interactions are found: the 2′-OH of the ribose of the Ado portion of NAD^+ engages in a hydrogen bond with Asp^{244}; the 3′-OH of the ribose of the Ado moiety of NAD^+ binds to a main-chain carbonyl oxygen of Tyr^{220}; the oxygen atoms of the pyrophosphate portion of NAD^+ bind to Lys^{290} and Tyr^{431}; the 2′-OH and 3′-OH of ribose of the Nic portion of NAD^+ are involved with Asn^{331}; and the carboxyl group of Nic is hydrogen-bonded to His^{428} (Fig. 2).

(2) Potential active-site structure

Using chemical modification methods, Gomi et al. [40] suggested that the active site of AdoHcy hydrolase contains a His residue [41], an Arg residue [42] and two Cys residues [43] which are required for the catalytic activity. A carboxyl group [44], which we postulated to be associated with an Asp or Glu residue, is probably involved in the abstraction of the 4′-H of the oxidized substrate. After comparing our model structure with the active-site structural information described above, we would like to propose that these residues correspond to His^{428} and Arg^{430}; the Cys^{78} and Cys^{112} residues could not be identified in our model. In the vicinity of the 4′-H of substrates (AdoHcy and Ado), no other basic amino acid residue could be identified except Asp^{427}, which is involved in hydrogen-bonding with the 3′-OH of substrates or inhibitors.

(3) Binding of substrates and inhibitors

The binding of AdoHcy is similar to the binding of Ado and Hcy, but slightly different from the binding of inhibitors. In the adenine portion of substrates and inhibitors, the 6-NH_2 group interacts with the main-chain carbonyl group of Leu^{329}, while in the inhibitors, the N(1) and N(3) atoms are also involved in hydrogen-bonding with Ser^{354} and Ser^{358}, respectively. Details of these interactions are given in Table 4 and Figs. 6–10. Since all the inhibitors contain a cyclopentenyl ring or cyclopentanyl ring instead of a ribose, the binding of the 3′-OH to Asp^{427} is different from that of AdoHcy and Ado. The relative binding energies of substrates or inhibitors in model complexes, as expressed by the YETI force field, are given in Table 5. The relative energy of the interaction between the model and inhibitors suggests that AristM and NpcA bind to AdoHcy hydrolase more strongly than do the rest of the inhibitors. Compound 7a (Table 6) binds to the models containing both NAD^+ and NADH. Compound 7b (Table 5) binds to the enzyme–NAD^+ complex much more weakly than does compound 7a. The RMS shifts of all α-carbon atom positions between LDH and model complexes of AdoHcy hydrolase (Table 3) are less than 0.7 Å; the largest maximum shift is 1.63 Å.

TABLE 4
HYDROGEN-BOND INTERACTIONS OF AdoHcy HYDROLASE AND SUBSTRATES AND INHIBITORS

Hydrogen-Bonding	H···Acc[a] distance (Å)								
	AdoHcy	Ado	NpcA	1	2	AristM	3	4	5
NH2---O=C- Leu[329]	1.9	2.7	1.9	1.9	1.9	1.9	2.0	2.0	2.2
N(1)---H-O- Ser[354]	3.2	5.5	1.9	1.9	1.9	1.9	1.9	1.9	1.9
N(3)---H-O- Ser[358]	3.8	4.2	1.9	1.9	2.0	2.0	2.0	2.1	2.3
2'OH---O-C- Asp[427]	6.4	1.8	2.4	2.5	2.7	2.0	2.1	2.1	2.6
2'OH---O	7.3	3.3	1.8	1.8	1.8	3.4	2.8	2.6	2.4
3'OH---O-C- Asp[427]	1.8	2.1	3.3	3.4	3.8	1.8	2.5	2.7	3.0
3'OH---O	3.4	4.0	1.8	1.8	2.4	2.5	1.8	1.8	1.8
5'OH---O-C- Asp[427] O	–	–	2.6	–	–	1.8	–	–	–
5'O---H_3N^+-Lys[425]	–	–	2.2	–	–	2.6	–	–	–
	Distance between 3'H of substrates or inhibitors and C4 of NAD^+ (Å)								
d(3'H-C4)	3.5	2.2	4.0	4.0	4.4	3.4	4.0	4.1	3.9
	Angle of N3-C4 (of NAD^+)-3'H or-3'C (of substrates and inhibitors) (deg)								
∠N3-C4-3'H	89	111	52	50	44	56	55	54	51
∠N3-C4-3'C	80	114	65	63	56	68	62	65	63

[a] Acc represents the hydrogen-bond acceptor.

DISCUSSION

(1) Generation of a model of the NAD^+ binding domain and active site for AdoHcy hydrolase

Using the software MUTAR, we derived a partial structure for AdoHcy hydrolase which includes the NAD^+ binding domain and the binding site for substrates (AdoHcy or Ado and Hcy) or inhibitors (e.g., NpcA). This partial structure of AdoHcy hydrolase was generated based on the 3D structure of LDH using the homology that exists in the primary sequence of these proteins. Our modeling approach is based on the role of NAD^+, which is involved in a redox reaction, and the similarity in the NAD^+ binding domains of the proteins mentioned in the Introduction section. The program MUTAR conserved the secondary structure of the NAD^+ binding domain, but changed the available space for the NAD^+ binding domain in some aspect due to differences in the amino acid side chains. For example, introducing a larger amino acid side chain (e.g., changing valine to phenylalanine) would change both the size and characteristics of the hydrophobic pocket for binding of the adenine portion of NAD^+. These differences present a problem in docking the NAD^+ into its binding domain. Although we knew that NAD^+ is tightly bound to AdoHcy hydrolase, we lacked knowledge about its conformation in the native enzyme. Nevertheless, we retrieved the NAD^+ molecule from the (*S*)-lac-NAD^+–LDH complex, and prerefined it using averaged parameters from the extended form of NAD^+ observed in X-ray studies [45]. This refined NAD^+ structure was then docked into its binding domain.

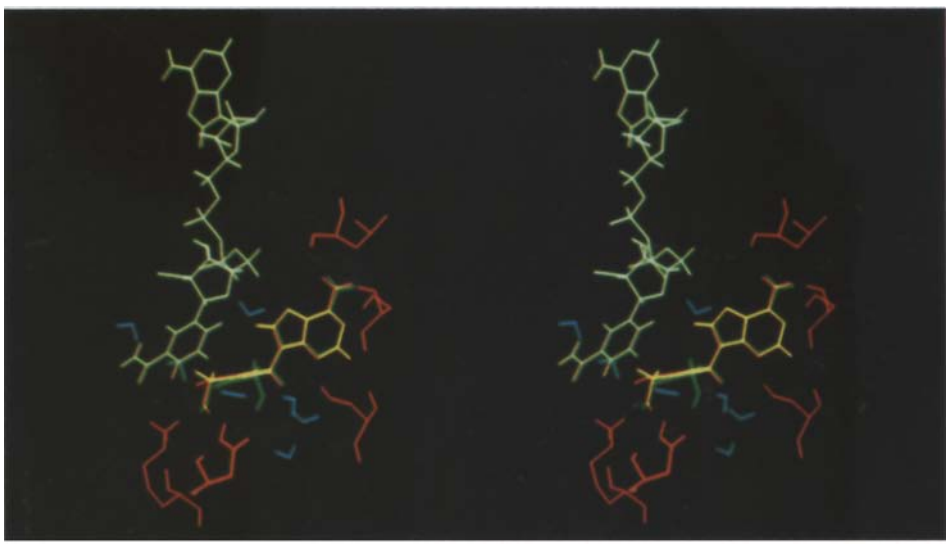

Fig. 10. Binding of compounds 7a (green) and 7b (red) in the active-site model of AdoHcy hydrolase containing NAD^+ (yellow) and NADH (light blue) and H_2O molecules (blue). Amino acid residues involved in binding of these compounds are red.

TABLE 5
RELATIVE BINDING ENERGIES OF SUBSTRATES AND INHIBITORS TO THE MODEL OF AdoHcy HYDROLASE

Compound	Enzyme form	Binding energy (kcal/mol)	K_m(μM)[a]	K_i(nM)[b]
AdoHcy	NAD^+	−73.5	15.2	–
Ado + Hcy	NAD^+	−75.4	1.05, 155	–
NpcA	NAD^+	−39.4	–	< 3[b]
AristM	NAD^+	−34.5	–	< 3[b]
1	NAD^+	−29.7	–	49[c]
2	NAD^+	−25.9	–	9150[c]
3	NAD^+	−31.4	–	12[c]
4	NAD^+	−30.1	–	27[c]
5	NAD^+	−27.9	–	5020[c] (1000)[d]
6	NAD^+	−31.3	–	22[c] (15)[d]
7a	NAD^+	−33.8	–	800[e]
7b	NAD^+	−29.4	–	800[e]
7a	NADH	−30.6	–	–
7b	NADH	−28.6	–	–
8	NAD^+	−29.1	–	84[c] (158)[d]

[a] K_m values are for the rat liver enzyme [1].
[b] An upper limit for K_i has been presented. Because of the potency of NpcA and AristM, it has been difficult to measure an accurate K_i value for these compounds.
[c] K_i values are for bovine liver enzyme [Wolfe et al., J. Med. Chem., submitted].
[d] Numbers in parentheses are calculated from the binding energy using the plot shown in Fig. 12.
[e] K_i values of 3′-ketoNpcA (mixture of 7a + 7b) were determined for bovine liver enzyme [54].

(2) Evaluation of computer-generated model structure

To evaluate the validity of the NAD^+ binding domain of AdoHcy hydrolase, we applied the following tests: (1) comparing the model structure with known structures of other dehydrogenases (e.g., the LDH–NAD^+ complex) and with other model structures of dinucleotide binding proteins (e.g., the p^{21} protein) [46, 47]; (2) comparing the structural information obtained from the binding of small molecules (e.g., substrates and inhibitors) with the available kinetic data; and (3) analyzing the utility of the model for rational drug design.

(a) Comparison of the model structure with the LDH–NAD^+ complex. From our model study, the structure of NAD^+ in AdoHcy hydrolase has an extended conformation with both Ado and Nic in anti-orientation. This conformation is similar to the conformation of NAD^+ in the NAD^+–LDH complex [45]. A comparison of NAD^+ binding in both enzymes is given in Table 6. Adenine binds in hydrophobic areas of AdoHcy hydrolase and LDH, and these hydrophobic areas appear to be fairly nonspecific. The 2′-OH group of the Ado portion of NAD^+ binds to an Asp residue in both enzymes. The 3′-OH group of the Ado moiety of NAD^+ binds a main-chain carbonyl oxygen of Tyr^{220} of the AdoHcy hydrolase model. In the NAD^+–LDH complex, it was reported that this 3′-OH group interacts with Asp^{30} [48]. In our model, the oxygen atoms of the pyrophosphate portion bind to AdoHcy hydrolase in the following fashion: one oxygen atom near the Ado portion is bound to the $-NH_3^+$ group of Lys^{290}, while another oxygen atom near Nic is bound to the –OH group of Tyr^{431}. This binding is different from what is observed in the NAD^+–LDH complex, where two oxygens from two phosphates were bound to the same amino acid residue, arginine, resulting in a conformational change in LDH [48]. The 2′-OH and 3′-OH groups of the sugar portion in the Nic fragment are bound to the main-chain imino group and NH_2 of the side chain of Asn^{331} in our model, while in the NAD^+–LDH complex they were bound seperately to asparagine and a main-chain carbonyl group. The carbonyl group of Nic interacts with His^{428} in our model, but interacts with lysine in the NAD^+–LDH complex.

(b) Comparison of the model structure with the p^{21} protein. When we compared our model structure with a model structure of the p^{21} protein [46], some similarities in the β–α–β fold of the dinucleotide binding region were found: (1) a hydrophobic core composed of Val^{214}, Val^{216},

TABLE 6
BINDING OF NAD^+ IN LDH [48] AND AdoHcy HYDROLASE MODEL

Functional Group of NAD^+	Amino acid residues in	
	LDH[a]	AdoHcy hydrolase
N(1) of adenine	(–OH) Tyr^{85}	–
–2′OH (Ado)	($-CO_2$) Asp^{53}	($-CO_2$) Asp^{244}
–3′OH (Ado)	($-CO_2$) Asp^{30}	(O=C<) Tyr^{220}
–P=O (Ado)	($-NH_2$) Arg^{101}	($-NH_3^+$) Lys^{290}
–P=O (Nic)	($-NH_2$) Arg^{101}	(–OH) Tyr^{431}
–2′OH (Nic)	(H–N<) Asn^{138}	(H–N<) Asn^{331}
–3′OH (Nic)	(O=C<) Ala^{98}	($-NH_2$) Asn^{331}
>C=O (Nic)	($-NH_3^+$) Lys^{250}	(–NH) His^{428}

[a] The numbering of the amino acid residues is different from that in the amino acid sequence of LDH [20].

Ala^{228}, Leu^{231}, and Ile^{240} in the AdoHcy hydrolase model corresponded to Leu^{6}, Val^{8}, Leu^{19}, Gln^{22}, and Val^{29} in the p^{21} protein; and (2) a salt linkage occurred between Lys^{225} and Glu^{242} in the AdoHcy hydrolase model, while in the p^{21} protein it was formed by Lys^{16} and Glu^{31}. In our model, this Lys^{225} can also form a stronger salt linkage with Glu^{254} and Glu^{257} than with Glu^{242}.

(c) Comparison of the model structure with the result of mutagenesis of AdoHcy hydrolase. We also compared our model with the result of the mutagenesis at the putative NAD^+ binding site of rat liver AdoHcy hydrolase [49]. The mutation of Gly to Val in the fingerprint sequence, Gly^{219}-X_{aa}-Gly^{221}-X_{aa}-X_{aa}-Gly^{224}, of the β–α–β fold has been shown to disrupt the formation of tetrameric AdoHcy hydrolase and prevent the binding of NAD^+; consequently, a loss of catalytic activity was observed [49]. In a preliminary study using our model, we observed that replacement of Gly^{219} by Val resulted in too short a distance (1.1 Å) between the γ-carbon atom of Val^{219} and the H atom attached to the C1′ of ribose of the Ado portion of NAD^+. We plan to extend this study to evaluate the influence of the mutations of Gly^{221} and Gly^{224} in NAD^+'s binding by means of molecular modeling.

(d) Comparison of substrates binding with kinetic data. Based on our model, we propose that Asp^{427} plays an important role in triggering the reaction catalyzed by AdoHcy hydrolase. In the catalytic mechanisms, the Asp^{427} could accept the H^+ from the 3′-OH group of the substrate when it is oxidized to 3′-keto (step 2 in Scheme 2) and the enzyme-bound NAD^+ is reduced to NADH with the H^- transferred from C3′ of substrate to C4 of Nic of the NAD^+. Although the redox step is not rate-limiting [50], the distance between the C3′ proton (3′H) of the substrates (sub), Ado or AdoHcy, or inhibitors (inh) and the C4 of NAD^+ and the angle of N1-(Nic)-C4(Nic)-3′H(sub or inh) may be important in order for a redox reaction to occur [51]. Thus, we used the X-ray crystal structure of Ado [52] to demonstrate that the distance from the 3′H of Ado to the C4 of Nic is 2.20 Å and the distance from the H atom of 3′-OH to the O atom of the carboxyl group of Asp^{427} is 2.08 Å. The angle of N1(Nic)-C4(Nic)-3′H(Ado) is 111°. In this case, the conformation of Ado and the model complex (Fig. 11) is slightly different from the AdoHcy-model complex (Table 5), but would allow the H^+/H^- transfer in forming an intermediate complex (3′-ketoAdo and NADH). A similar orientation with an angle of 103° for N1(Nic)-C4(Nic)-3′H(sub) and a distance of 2.3 Å between the reactive hydrogen and C4 of Nic has also been observed in alcohol dehydrogenase when its substrate, cyclohexanol, is bound [53].

(e) Comparison of inhibitors binding with available kinetic data. The ability of the inhibitors to bind in model complexes is consistent with their inhibitory effects [5, 10–12 and Wolfe et al., J. Med. Chem., submitted]. NpcA is a potent inhibitor of AdoHcy hydrolase; it inhibits the enzyme by being converted into 3′-ketoNpcA (a mixture of compounds 7a + 7b) with subsequent conversion of NAD^+ to NADH [3]. Our laboratory has successfully isolated the 3′-ketoNpcA (compounds 7a + 7b) [54], and we have also demonstrated by molecular modeling that this molecule, either in the keto (7a) or enol (7b) form, can bind to the model structure containing NAD^+ (Fig. 10). Our model studies did not prove that the keto form 7a binds to the NADH form of the enzyme better than it binds to the NAD^+ form of the enzyme. However, our model did show that enol form 7b binds to the enzyme–NAD^+ complex less tightly than the keto form 7a (Table 5). This may be important because the enol form 7b in solution may be the predominant form of this molecule. The 3′-ketoNpcA (7a + 7b) is a weak inhibitor of the NAD^+ form of AdoHcy hydrolase [54].

Compounds 1 and 2 and compounds 3 and 4 are analogs of NpcA and AristM, respectively.

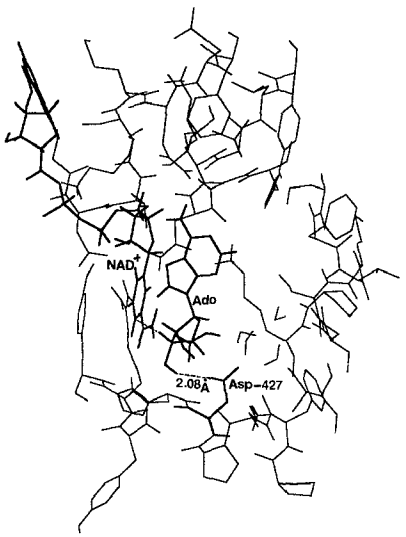

Fig. 11. Binding of Ado (X-ray crystal structure) in the active-site model of AdoHcy hydrolase. Bold lines represent NAD^+, Ado and Asp^{427}. The distance between the C4 of NAD^+ and 3'H of Ado is 2.20 Å (dashed line), while the distance between the H atom of the 3'OH group in Ado and the carbonyl oxygen atom of Asp^{427} is 2.08 Å (dashed line).

These analogs were designed to prevent the phosphorylation of the 5'-OH of NpcA and AristM, which causes the cytotoxicity of NpcA and AristM in murine L929 cells [11, 12]. The observed K_i values of these inhibitors correlate with their binding strengths to the model of AdoHcy hydrolase. The relative binding energies of inhibitors with the model (Table 5) can be used to obtain a linear relationship with the values of $\log(K_i)$ (Fig. 12). In all cases, the order of activity is: NpcA $\geqslant$ AristM > 3 > 4 > 1 >> 2. Compound 1 binds to the model in a manner similar to NpcA (Fig. 7), while compound 2 binds in a different way. The main difference is in the binding of the 3'-OH toward Asp^{427} (Table 4). Compounds 3 and 4 bind to the model in much the same way as AristM (Fig. 8). We feel that the orientation of 3'-OH toward Asp^{427} and the pK_a values of 3'-OH in inhibitors could be important factors in determining their potency.

(f) Analyzing the utility of the model for rational drug design. Since the synthetic efforts in our laboratory have been devoted toward making carbocyclic analogs lacking the 4'-hydroxymethyl group [10–12], we were interested in determining how this functional group interacted with the computer-generated AdoHcy hydrolase model. Because of the potent inhibitor effects of NpcA and AristM, we suspected that there might exist a hydrophilic environment in the enzyme for binding the –OH of the 4'-hydroxymethyl group. In our model, this –OH group is oriented in such a manner that it can interact with the $-NH_3^+$ group of Lys^{425} via a hydrogen bond; thus, this interaction may contribute to the binding and explain the reduced binding ability of analogs lacking the 4'-hydroxymethyl group (e.g., compounds 1 and 3).

Having developed this AdoHcy hydrolase model and shown retrospectively that it can rationalize the inhibitory activity of compounds synthesized earlier in our program (e.g., compounds 1–4), we attempted to test the model by calculating the K_i values for three new inhibitors (e.g., compounds 5, 6 and 8) synthesized in our laboratory and comparing these values to experimentally determined values. As shown in Table 5, the model accurately predicted the K_i value of com-

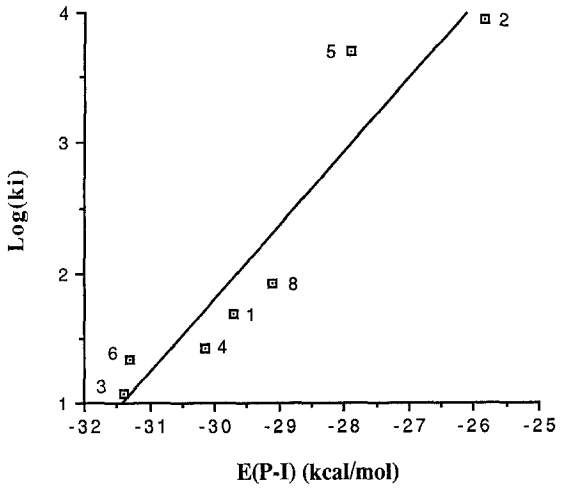

Fig. 12. Plot of E(P–I) vs. log(K_i). E(P–I) = binding energy of inhibitor to the active-site model of AdoHcy hydrolase; K_i = inhibition constant (Table 5); the correlation coefficient of the plot is 0.90.

pound 6 but underestimated the K_i value for compound 8 and overestimated the K_i value for compound 5. However, it should be noted that the model did predict the significant difference observed in the K_i values for compounds 4 and 5, which differ structurally only in the orientation of the 4′-methyl group (Fig. 8).

(3) Future studies

In our modeling studies, all inhibitors except compound 8 (Fig. 9) were assumed to have anti-conformations at the glycosyl bond when they are bound to AdoHcy hydrolase. These assumptions were based on preliminary studies, using nuclear magnetic resonance (NMR) spectroscopy, in which we found that compound 1 has an anti conformation in DMSO/D_2O solution and compound 3 has an anti-conformation in DMSO solution [Yeh et al., unpublished results]. We constructed compound 8 with the syn-conformation since it would give a better affinity to our model structure.

In addition to the issue of syn- and anti-conformation at the glycosyl bond, there are other structural features of the substrate and inhibitors which need to be defined (e.g., conformation of carbocyclic ring). The refined guest–host complexes may, however, represent a local energy minimum. As in all molecular mechanics-type calculations, the problem of obtaining 'only' a local minimum structure is possible. The structures obtained by our methods represent a possible conformation which is in agreement with structural data retrieved from the CSD and the BPDB. To prevent the structure from being trapped in a local energy minimum, we are pursuing two different approaches: (1) obtain the structural information from NMR studies with small molecules in solution; and (2) perform molecular dynamics simulations [55]. We plan to conduct the conformational study on all inhibitors by NMR, since the activity of these inhibitors may be related to their conformation in solution, which may be useful in evaluating our model. We are also currently engaged in studying the solvation of inhibitors with Monte Carlo water by molecular mechan-

ics as well as by molecular dynamics simulation. The latter technique will also be applied to our model complex.

CONCLUSIONS

Using the primary sequence of rat liver AdoHcy hydrolase and tertiary structure of LDH and the homologous protein modeling approach, we obtained a model for the active site of AdoHcy hydrolase. Presently, no X-ray crystal structure of AdoHcy hydrolase exists that could be used to verify this model. However, we were able to correlate the bindings of inhibitors to our model with the data from inhibition studies of bovine liver AdoHcy hydrolase. This model has proven useful in predicting structures that would have either high or low affinity for the active site of this enzyme. It may also be useful for the enzyme isolated from other sources since it was recently reported that the sequence of human AdoHcy hydrolase shows 97% homology to the rat liver enzyme [56].

ACKNOWLEDGEMENTS

The authors would like to express their thanks to Professor Richard L. Schowen as well as to Mr. David W. Huhta and Dr. Tomi Joseph for valuable discussion. This work was supported by grants from the National Institutes of Health (GM-29332) and Glaxo, Inc.

REFERENCES

1 Ueland, P.M., Pharmacol. Rev., 34 (1982) 223.
2 Hohman, R.J., Guitton, M.C. and Veron, M., Proc. Natl. Acad. Sci. USA, 82 (1985) 4578.
3 Matuszewska, B. and Borchardt, R.T., J. Biol. Chem., 262 (1987) 265.
4 Keller, B.T. and Borchardt, R.T., In: DeClercq, E. and Walker, R.T. (Eds.), Antiviral Drug Development, Plenum Press, New York, 1988, pp. 123–138.
5 Borchardt, R.T., Keller, B.T. and Patel-Thombre, U., J. Biol. Chem., 259 (1984) 4353.
6 DeClercq, E., Antimicrob. Agents Chemother., 28 (1985) 84.
7 Keller, B.T., Clark, R.S., Pegg, A.E. and Borchardt, R.T., Mol. Pharmacol., 28 (1985) 364.
8 Guranowski, A., Montgomery, J.A., Cantoni, G.L. and Chiang, P.K., Biochemistry, 20 (1981) 110.
9 Montgomery, J.A., Acc. Chem. Res., 19 (1986) 293.
10 Narayanan, S.R., Keller, B.T., Borcherding, D.R., Scholtz, S.A. and Borchardt, R.T., J. Med. Chem., 31 (1987) 500.
11 Hasobe, M., McKee, J.G., Borcherding, D.R., Keller, B.T. and Borchardt, R.T., Mol. Pharmacol., 33 (1988) 713.
12 Hasobe, M., McKee, J.G., Borcherding, D.R. and Borchardt, R.T., Antimicrob. Agents Chemother., 31 (1987) 1849.
13 Birktoft, J.J. and Banaszak, L.J., In: Hearn, M.T.W. (Ed.), Peptide and Protein Reviews, Vol. 4, Marcel Dekker, New York, 1984, pp. 1–46.
14 Brändén, C. and Eklund, H., In: Jeffery, J. (Ed.), Dehydrogenase Requiring Nicotinamide Coenzyme, Birkhäuser Verlag, Basel, 1980, pp. 1–43.
15 Palmer, J.L. and Abeles, R.H., J. Biol. Chem., 254 (1979) 1217.
16 Kollman, P., Annu. Rev. Phys. Chem., 38 (1987) 303.
17 Gund, T. and Gund, P., In: Liebman, J.F. and Greenberg, A. (Eds.), Molecular Structure and Energetics, VCH, New York, 1987, pp. 319–340.
18 Frühbeis, H., Klein, R. and Wallmeier, H., Angew. Chem. Int. Ed. Engl., 26 (1987) 403.
19 Stewart, D.E., Weiner, P.K. and Wampler, J.E., J. Mol. Graphics 5 (1987) 133.
20 Taylor, S.S., J. Biol. Chem., 252 (1977) 1799.

21 Ogawa, H., Gomi, T., Mueckler, M.M., Fujioka, M., Backlund, P.S., Aksamit, R.R., Unson, C.G. and Cantoni, G.L., Proc. Natl. Acad. Sci. USA, 84 (1987) 719.
22 Kasir, J., Aksamit, R.R., Backlund, P.S. and Cantoni, G.L., Biochem. Biophys. Res. Commun., 153 (1988) 359.
23 Eventoff, W., Rossmann, M.G., Taylor, S.S., Torff, H., Meyer, H., Keil, W. and Kiltz, H., Proc. Natl. Acad. Sci. USA, 74 (1977) 2677.
24 White, J.L., Hackert, M.L., Buehner, M., Adams, M.J., Ford, G.C., Lentz, P.J., Smiley, I.E., Steindel, S.J. and Rossmann, M.G., J. Mol. Biol., 102 (1976) 759.
25 Bernstein, F.C., Koetzle, T.F., Williams, G.J.B., Meyer, E.F., Brice, M.D., Rodgers, J.R., Kennard, O., Shimanouchi, T. and Tasumi, M., J. Mol. Biol., 112 (1977) 535.
26 Singh, U.C., Weiner, P.K., Caldwell, J. and Kollman, P.A., Department of Pharmaceutical Chemistry, University of California, San Francisco, CA 94143.
27 Vedani, A. and Huhta, D.W., J. Am. Chem. Soc., 112 (1990) 4759.
28 Brooks, B.R., Bruccoleri, R.E., Olafson, B.D., States, D.J., Swaminathan, S. and Karplus, M., J. Comp. Chem., 4 (1983) 187.
29 Eklund, H., Samama, J.P., Wallén, L., Brändén, C.I., Åkeson, Å. and Jones, T.A., J. Mol. Biol., 146 (1981) 561.
30 Jones, T.A., In: Sayre, D. (Ed.), Computational Crystallography, Clarendon Press, Oxford, 1982, pp. 303–317.
31 Dewar, M.J.S. and Thiel, W., J. Am. Chem. Soc., 99 (1977) 4899.
32 Grau, U.M., Trommer, W.E. and Rossmann, M.G., J. Mol. Biol., 151 (1981) 289.
33 Still, W.C., Richards, N.G.J., Guida, W.C., Lipton, M., Liskamp, R., Chang, G. and Hendrickson, T., Department of Chemistry, Columbia University, New York, NY 10027.
34 Ishida, T., Tanaka, A., Inoue, M., Fujiwara, T. and Tomita, K., J. Am. Chem. Soc., 104 (1982) 7239.
35 Hayashi, M., Yaginuma, S., Yoshioka, H. and Nakatsu, K., J. Antibiot., 34 (1981) 675.
36 Kishi, T., Muroi, M., Kusaka, T., Nishikawa, T., Kamiya, K. and Mizuno, K., Chem. Pharm. Bull., 20 (1972) 940.
37 Allen, F.H., Bellard, S., Brice, M.D., Cartwright, B.A., Doubleday, A., Higgs, H., Hummelink, T., Hummelink-Peters, B.G., Kennard, O., Motherwell, W.D.S., Rodgers, J.R. and Watson, D.G., Acta Crystallogr., B35 (1979) 2331.
38 Jacober, S.P., SOLVGEN: An Approach to Protein Hydration, M.S. Thesis, Department of Computer Science, University of Kansas, Lawrence, KS, 1988.
39 Vedani, A., Huhta, D. and Jacober, S.P., J. Am. Chem. Soc., 111 (1989) 4075.
40 Gomi, T., Ogawa, H. and Fujioka, M., J. Biol. Chem., 261 (1986) 13422.
41 Gomi, T. and Fujioka, M., Biochemistry, 22 (1983) 137.
42 Takata, Y. and Fujioka, M., J. Biol. Chem., 258 (1983) 7374.
43 Takata, Y. and Fujioka, M., Biochemistry, 23 (1984) 4357.
44 Takata, Y., Gomi, T. and Fujioka, M., Arch. Biochem. Biophys., 240 (1985) 827.
45 Parthasarathy, R. and Fridey, S.M., Science, 226 (1984) 969.
46 Wierenga, R.K. and Hol, W.G.J., Nature (Lond.) 302 (1983) 842.
47 Wierenga, R.K., Terpstra, P. and Hol, W.G.J., J. Mol. Biol., 187 (1986) 101.
48 Holbrook, J.J., Lilijas, A., Steindel, S.J. and Rossmann, M.G., In: Boyer, P.D. (Ed.), The Enzymes, Vol. 11, Academic Press, New York, 1975, pp. 191–292.
49 Gomi, T., Date, T., Ogawa, H., Fujioka, M., Aksamit, R.R., Backlund, P.S. and Cantoni, G.L., J. Biol. Chem., 264 (1989) 16138.
50 Sinhababu, A.K., Bartel, R.B., Pochopin, N. and Borchardt, R.T., J. Am. Chem. Soc., 107 (1985) 7628.
51 Bürgi, H.B., Dunitz, J.D., Lehn, J.M. and Wipff, G., Tetrahedron, 30 (1974) 1563.
52 Lai, T.F. and Marsh, R.E., Acta Crystallogr., B28 (1972) 1982.
53 Horjales, E. and Brändén, C., J. Biol. Chem., 260 (1985) 15445.
54 Paisiley, S.D., Wolfe, M.S. and Borchardt, R.T., J. Med. Chem., 32 (1989) 1415.
55 McCammon, J.A. and Harvey, S.C., Dynamics of Protein and Nucleic Acids, Cambridge University Press, London, 1987.
56 Coulter-Karis, D.E. and Hershfield, M.S., Ann. Hum. Genet., 53 (1989) 169.